



PREPARING A COMPREHENSIVE ANALYSIS OF THE MECHANICAL CLASSIFICATION OF STRUCTURAL GLASS

Gergely Molnár^{1*}, László Milán Molnár², Imre Bojtár¹

¹Department of Structural Mechanics, Budapest University of Technology and Economics, Műegyetem rkp. 3. K mf. 45. Budapest, Hungary

²Department of Electronics Technology, Budapest University of Technology and Economics, Goldmann György tér. 3., V2, 2nd floor, Budapest, Hungary

*corresponding author: Tel.: +36 1 463-1345; e-mail: gmolnar@mail.bme.hu

Resume

Present study deals with the mesostructure analysis of the structural glass. The subject is about to prepare a comprehensive mechanical analysis, aimed on the understanding of the multiscale mechanical behaviour of soda-lime-silica glass used as an architectural element.

After a brief description of the micro and mesostructure of glass we will explain our goals in this analysis.

We have divided the glass plate – from a mesoscopic aspect – into three major regions. The first region is the external surface, which is the largest area of a plate. The effect of the surface imperfections is negligible due to a grinded edge finishing, so we considered the second region as the edge. The third region contains the inhomogeneities in the glass material itself. To describe the mesostructure we have done atomic force microscopy (AFM) and micro computed tomography (μ CT) scans. We used the AFM to image the surface and the edge and μ CT to collect geometrical information from the inhomogeneities.

The aim of the overall analysis is to develop a new certification procedure to qualify the structural glass in a mechanical a way.

Article info

Article history:

Received 29 January 2012

Accepted 8 March 2012

Online 10 March 2012

Keywords:

multiscale analysis;

defects;

AFM;

micro-CT;

inhomogeneities

ISSN 1335-0803 (print version)

ISSN 1338-6174 (online version)

Available online: <http://fstroj.uniza.sk/PDF/2012/12-2012.pdf>

1. Introduction

Glass is one of the most popular building materials nowadays. The material itself has a very high strength, but most of the design standards make very serious restrictions about the effective tensile strength of glass [1]. In Fig. 1 you can see the glasses effective tensile strength is the function of the effective crack length. That means if we look at a tempered structural glass plate, the effective tensile strength will be much lower than a glass fibers one. The explanation of this phenomena is in the amorphous structure of the material. Thanks to the atomic structure, the material is completely

brittle, a small flaw or inclusion causes a great stress peak in the materials structure.

It is essential to describe the mesostructure of the glass, to know the exact effect of the flaws and inclusions. That is the reason of the multiscale analysis. We built finite element models in ANSYS 13.0, using the data which was gathered with AFM (Atomic Force Microscopy), and μ CT (micro Computed Tomography).

During the article we will call the soda-lime-silica as glass (The English word glass originates from the Latin word *gleasum*, which means amber in English.)

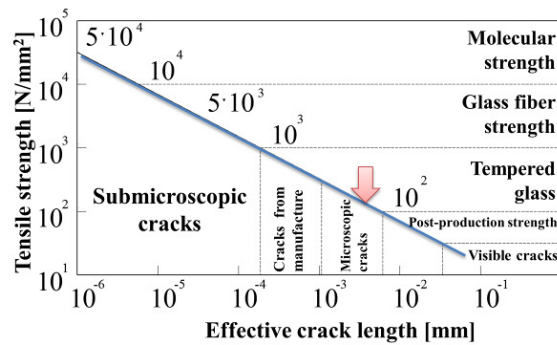


Fig. 1. Effective tensile strength in the function of the effective crack length [1]

2. Macroscale experiment

In a former experiment [2], we did a large scale, macroscopic investigation according to the standard EN 1288:3-2000 [4]. It is basically a four point bending test on laminated structural glass plates. During the experiment we measured the deflections and the strains in the middle region. There were strain gauges on the upper and on the lower glass plates.

We can see that the effective tensile strength was approximately 160 MPa, according to the measurement. The strength data had a 10.66 % standard deviation, (Table 1).

Table 1
Effective tensile strength calculated from the measured strains

Layer structure [mm]	Measured effective tensile strength [N/mm ²]
6 - 0.76 - 6	168.59
6 - 1.52 - 6	180.23
10 - 0.76 - 10	165.55
10 - 1.52 - 10	134.00
10-0.38-10-0.38-10	152.00
Average	160.07
Standard deviation	17.70
Relative standard deviation	10,66 %

In almost every case the first fracture manifested very close to the edge. We would like to explain the results with the mesoscale investigation. In this article we will show the methods we used to describe the mesostructure of the glass and some preliminary results.

We received the specimens from two companies. The inclusions were provided by Guardian Hungary Co. Ltd., the edge pieces were provided by OROSHÁZA GLAS Ltd. We have received surface specimens from both companies too.

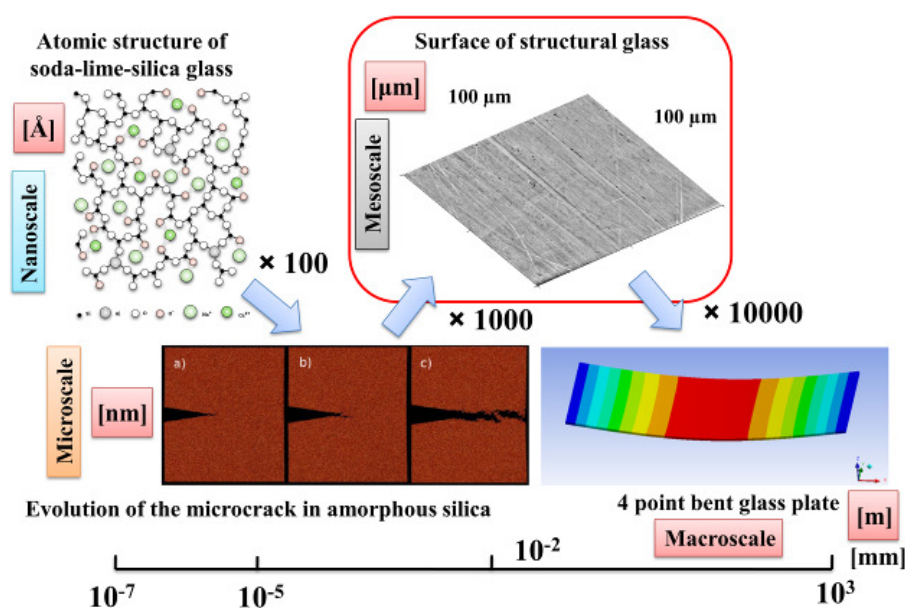


Fig. 2. Schematic figure of the multiscale approach
(Full colour version available online)

3. Multiscale concept

What is multiscale analysis anyway?

In Fig. 2 you can see four levels of the material glass. The first level is a nanoscopic problem, here we have to calculate the bounding energies of the molecular structure. This analysis can be done by using molecular dynamic simulations. We could use the same method to investigate a dynamic microcrack evolution in amorphous silica, done by Rountree et. al. [5].

But we always want to reach a macroscopic level, which can be used by practicing engineers. Also a mesoscopic approach can develop a mechanical certification for architectural glass. The industry can classify the product in not only an optical, but a mechanical way. To connect the micro and the macro level, we have to do another type of analysis. This is the mesoscopic investigation.

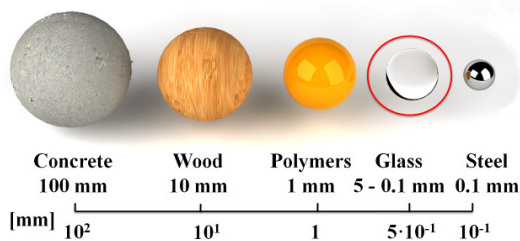


Fig. 3. Positioning the glasses RVE
(Full colour version available online)

Before we begin, we must define the RVE for the glass. The RVE is a Representative Volume Element which contains all the relevant mechanical properties of the material, which we would like to analyse. According to our investigation, for a mesoscopic analysis we could put the glasses RVE between 0.1-5 mm (Fig. 3). All the inhomogeneities must be much smaller than the RVE, but the RVE must be also smaller than a macroscopic structural element.

Let's consider a glass plate. First we have to divide the plates into regions. The first region is the surface (AFM image). You can see in Fig. 4 that the surface is full with microscopic flaws and scratches. The second region is the edge. The edge can be processed in many ways. My investigation is only extended to grinded

and polished edges. We didn't consider sand blasted glass surfaces. The third region is the most difficult part, the inclusions.

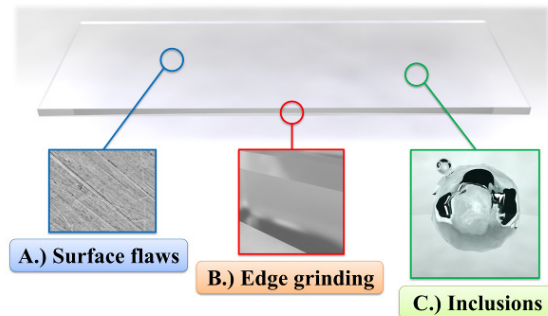


Fig. 4. Glass plate mesoscopic regions
(Full colour version available online)

4. Measuring techniques

To describe the mesostructure of the material, we have used two techniques. To map the topology of the surface and the edge we have used AFM (Atomic Force Microscopy). To measure the inclusions we have used μ CT.

4.1. Scanning Electro Microscopy (SEM)

We have used Inspect™ S50 Scanning Electron Microscope. The pressure was 5×10^{-4} Pa in the sample chamber with 20 kV accelerating voltage. The microscope could reach 100 000 fold magnification with a very large depth of field.

4.2. Atomic Force Microscopy (AFM)

Before we started the surface and the edge examination, we made SEM (Scanning Electro Microscopy) images of the specimens. We have decided, that the edge is so uneven, that it does not need any preparation before the AFM test. But the glass surface was very smooth, so we have decided to clear the surface with the procedure based on the recommendation of [6] to make the microflaws visible. The procedure is used to clear biosensor surfaces [7] as well.

The surface specimens were immersed into a 1:1:5 (volume) mixture of 25% ammonia (NH_3OH), 30 % hydrogen peroxide (H_2O_2) and water. The mixture was heated to 80 °C, and the specimens was in the liquid for 5 minutes. The first step removed all organic compounds, and some of the light metals. The second step was to

treat the surface with the 1:1:5 volume mixture of 37.5 % hydrochloride (HCl), 30 % hydrogen peroxide (H₂O₂) and water. The second mixture was also heated to 80 °C. The specimens were in the mixture for 5 minutes.

After the chemical bath, the glass surfaces were rinsed twice with hydrogen peroxide, methanol, dichloromethane and diethyl ether. All the residual diethyl ether was removed with nitrogen gas before the AFM imaging.

According to [6] the cleaning procedure did not etched the surface in this short period of time.

Contact atomic force microscopy is based on a very sensitive spring (called cantilever), which ends in a sharp tip. This tip is pushed down to the surface of the sample with a well-defined lateral force. Then, the sample is moved by a precise piezoelectric scanner in the x and y lateral directions. The image builds up from vertical deflection of the cantilever, which is measured by laser reflection. The laser beam is reflected on the cantilever, and gets into a four-segment photodetector (see Fig. 5).

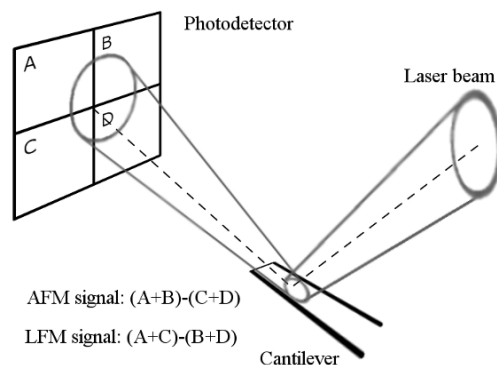


Fig. 5. Schematic of laser reflection in AFM optical unit [8]; Veeco diInnova multi-purpose SPM (Full colour version available online)

For practical considerations, the z (height) data does not come from the photo-voltage itself, but from a PID feedback loop. This loop connects the signal of the photodetector, and the third, vertical axis of the piezoelectric scanner. If the laser indicates that the deflection changed compared to a reference photo-voltage (called set-point), showing that the tip, and the cantilever moves up or down, the piezoscanner will move in the opposite direction, creating a negative feedback loop. The z information originated from the z driving signal of the piezo. We used Veeco Innova universal SPM (Scanning Probe Microscopy) instrument for AFM investigations.

For contact mode AFM, very high sensitivity silicon-nitride probes were used with average spring constant of 0,06 N/m.

4.3. Micro Computed Tomography (μ CT)

To measure the inhomogeneities we have used μ CT. Micro Computed Tomography (microCT or μ CT) is basically a commonly used 3D medical imaging technique. It makes 2D X-ray images then with a special software we could reconstruct a 3D model of the specimen.

The images are made by one or more detectors. While the X-ray source is moves around the specimen the detector makes images in 5 degree steps. After the recording, the computer reconstructs the segments of the object, which can be used to build a 3D volume. After the analog-to-digital conversion in the memory the raw data becomes a digital matrix, where each element of the matrix represents the X-ray attenuation ability of a voxel [9]. A special measure, the Hounsfield Unit (HU) represents the X-ray absorption capability of a material, which is a standardised and accepted unit to measure a materials X-ray attenuation compared to the water and the air. The absorption coefficient is a material property, it depends on the atomic numbers of the components, the density, and the frequency of the X-ray. The attenuation value for the air is -1000 HU by definition, for water it is 0 HU. For

a material X with linear attenuation coefficient μ_x , the corresponding HU value is therefore given by:

$$HU = \frac{\mu_x - \mu_{H_2O}}{\mu_{H_2O} - \mu_{air}} \times 1000 \quad (1)$$

where μ_{water} and μ_{air} are the linear attenuation coefficients of water and air, respectively. Thus, a change of one Hounsfield unit (HU) represents a change of 0.1% of the attenuation coefficient of water since the attenuation coefficient of air is nearly zero. It is the definition for CT scanners that are calibrated with reference to water.

The applied μ CT is a cone beam computed tomography (CBCT). CBCT is commonly used in dentistry. During a CBCT scan, the scanner rotates around the patient's head, obtaining up to nearly 600 distinct images. CBCT uses conical beam to make a series of 2D X-ray images.

The μ CT generates a very high resolution image. We used 60 kV accelerating energy, and reached 6 μ m size voxels.

In order to avoid unnecessary distortion, we prepared the specimen in a column shape,

because this way the radiation has to pass the least amount of glass.

We have assumed that the images made by μ CT are the exact representation of the specimens.

5. Results

In this paragraph we will show the microscopic results, and some further preparation to make the microscope data into a finite element geometry.

The inclusions had a prolate spheroid shape and its position was parallel with the glass surface so we could construct the geometry in ANSYS 13.0 Workbench easily.

With the AFM data we were not so lucky. The AFM data is a large matrix, each element contains the data of a specified points height. We wrote conversion software in Visual Basic to convert the AFM data to ANSYS geometry. During the numerical analysis we used prescribed displacements as boundary conditions.

In each case we built a reference model, without any imperfections – it had no strain peak. After the numerical calculation we have compared the strain peaks of the perfect reference volume and the real model. Some results are presented below.

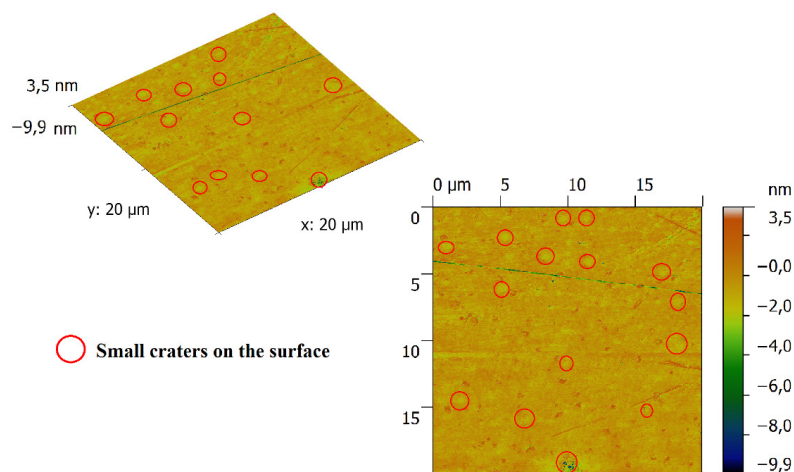
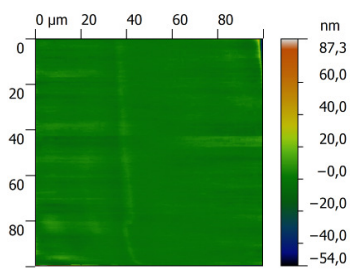
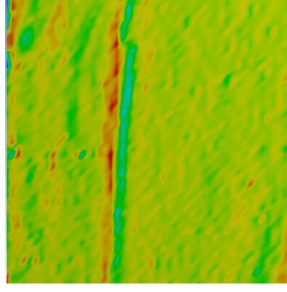
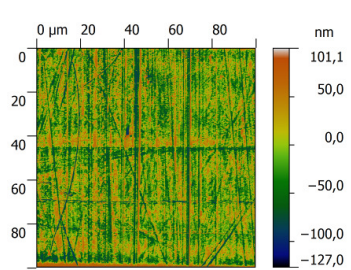
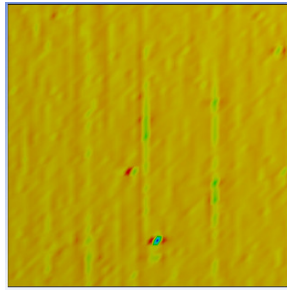
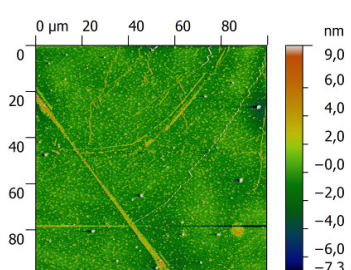
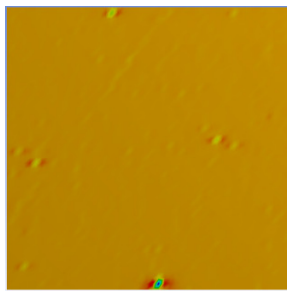
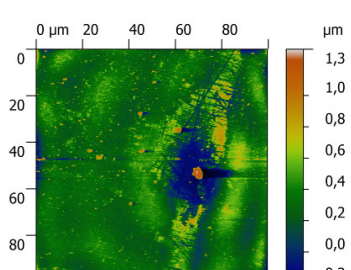
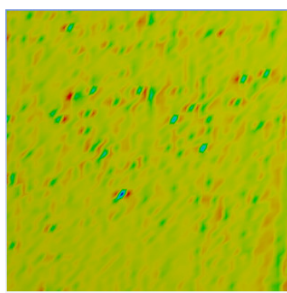
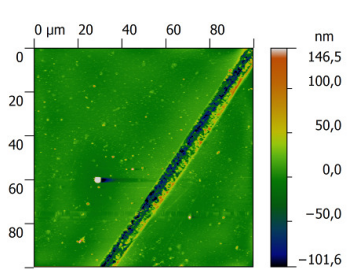
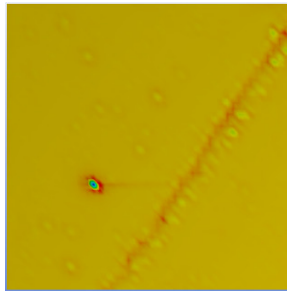


Fig. 6. Surface topology of a 1 year old glass specimen
(Full colour version available online)

Table 2

<i>Results on the surface (Full colour version available online)</i>			
	AFM images	FEA results	Strain peaks
After production			+7.80 %
After processing			+36.59 %
After 1 years of use			+44.41 %
After 3 years of use			+70.11 %
After 15 years of use			+97.06 %

5.1. Surface flaw analysis

On the glass specimen directly after the production (Guardian Hungary Co. Ltd.) only a few very shallow scratch could be recognised, but they are only a few nanometres deep.

In the second column the specimen was taken after the processing factory (OROSházaGLAS Ltd.). The surface of the specimen is full of nanoflaws. In the third column, a glass surface can be seen after being used for three years as a facade. The nanoscratches vanish, but small pits appear. In the images taken from the numerical calculations small pits could be recognised which generate the major strain peaks. In Fig. 6 you can see an AFM image and a 3D topology reconstruction of a 1 year old specimen. It could be recognised that the surface is full of small, shallow craters, presumably made by the weather. In Fig. 7 you can see that the strain peak rising takes place in the first few years. According to the numerical simulations made of the AFM data the rising could be approximated with a power function. On the youngest specimen, there is almost no strain rising (7.8 %), but if we consider an older one, the +70.11 % (facade - we have received the specimen and the information about the specimen from Associate Professor László Horváth (Department of Structural Engineering, Budapest University of Technology and Economy)) or the +97.06 % rising could be relevant (Table 2). (We have received the older specimens from Ku-Pa Üvegipari Ltd.)

5.2. Edge grinding

The grinded edge had a rougher texture than the polished one (SEM images in Table 3, row 1). The strain peaks on the edge are more conspicuous than on the surface. Numerical test showed that on the grinded edge the maximum strain peak was approximately +350 % larger compared to the reference volume. The relative standard deviation was approximately 10 % in all cases. At the main experiment we got almost

the same value (Table 1)

Our calculation shows that according to the numerical test, we can double the effective tensile strength by polishing the edges.

If we look at the results in the 2nd column (Table 3) we could recognise that the acid etched surfaces could cause similar strain peaks as a grinded edge. Usually we etch the surface with acid, not the edge. In the previous section we can see that the maximal strain peak could be +70 % on untreated, ordinary surfaces but if we treat the surface with acid, it could rise to +330 %, which is a great concern about the considerable effective tensile strength.

5.3. Inclusion caused strain peaks

We used Skyscan 1172 μ CT to describe the geometry of the inhomogeneities in the glass. We made images from six bubbles and one stone – received from Guardian Hungary Co. Ltd. You can see bubbles in different sizes on Fig. 9. The figure shows that these defects appear in different size and slightly different shapes.

The specimens were prepared in an efficient column shape for the test. The bubbles were easy to recognise (Fig. 8) because they had no attenuation value.

However the stones are imperfectly melted material compounds, so they had similar density as the glass. (Fig. 10)

We used the same prescribed displacements on the RVE with the inclusions – perpendicular tension (X direction) to bubble, parallel tension (Y direction) to the bubble and tension in both directions.

Table 4 shows the results of a void placed in the glass. In the Figures in Table 4 you can see, that a few millimeter size bubble could generate a great strain peak in the glass, so more work is needed in this case.

Therefore we need the statistical distribution of the inhomogeneities. We need information about the position, and the quantity of the inclusions.

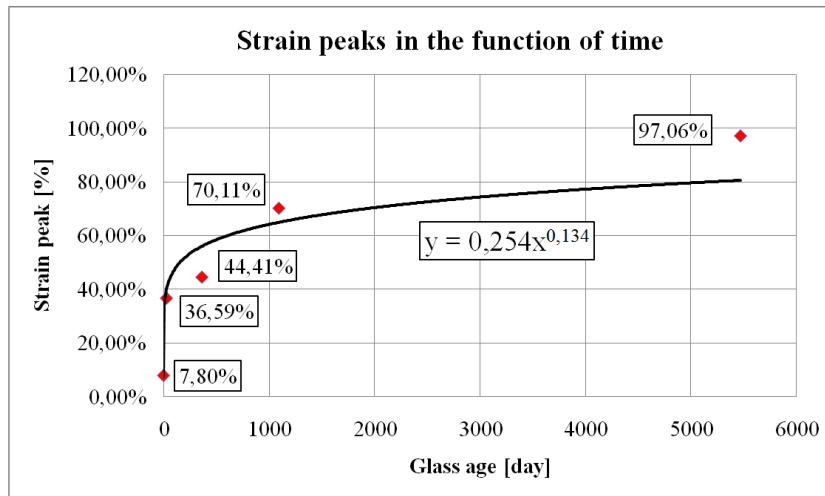


Fig. 7. Strain peaks in the function of ageing

Table 3

Results on the edge (Full colour version available online)

	Grinded	Acid etched	Polished edge
SEM images			
AFM images			
FEA results			
Maximum strain peaks	+352.46 %	+333,43 %	+206.40 %
Average	+291.38 %	+292,14 %	+153.88 %
Relative deviation	9.49 %	7.19 %	9.36%

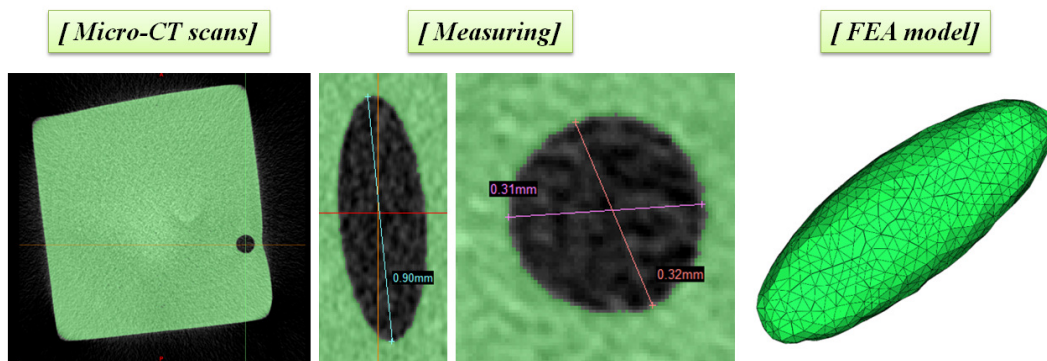


Fig. 8. Building FEM geometry of a bubble using μ CT
(Full colour version available online)



Fig. 9. Bubbles in glass

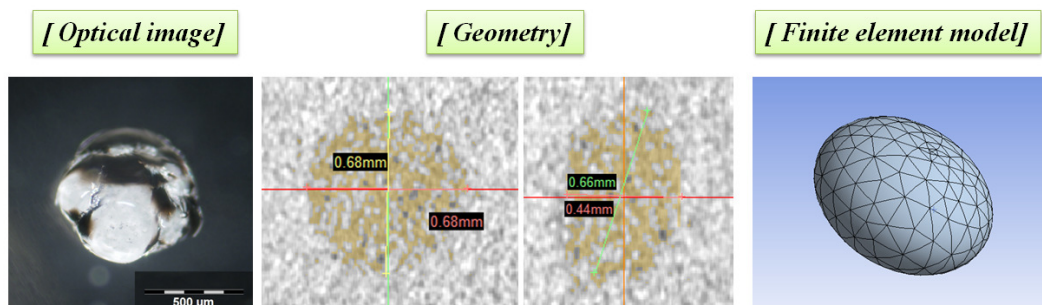
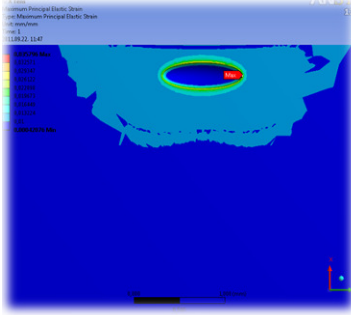
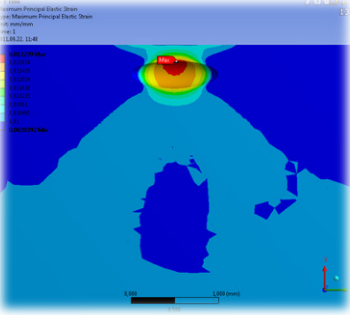
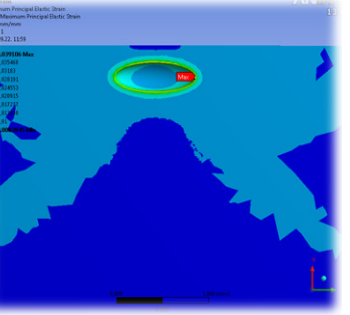
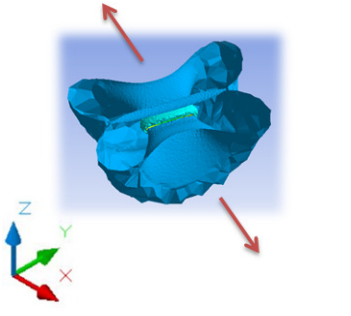
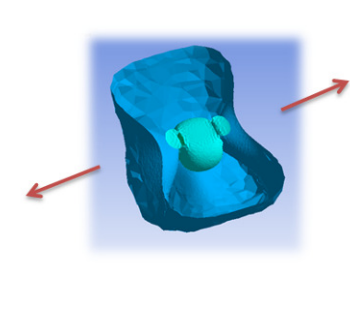
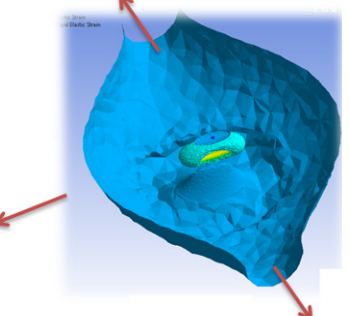


Fig. 10. FEM geometry of a stone using μ CT
(Full colour version available online)

Table 4

Results on the inclusions (Full colour version available online)

	X dir. tension	Y dir. tension	Two dir. tension
Maximal principal strain			
Strain capsules			
Strain peak	+257.96 %	+32.39 %	+291.06 %

With statistical information of the distribution and the geometry we could perform defect analysis using homogenisation schemes.

With the analysis are able to determine the mechanical effect of the inclusions in structural glass. We will be able to define a size effect coefficient which refers to the defects not on the surface but in the glass inner structure. It is relevant because structural glass is used in tempered form, so a special tension stress distribution appears inside the glasses volume.

With the calculated data we can prevent premature failure and the production process could be improved.

6. Conclusions

The microscopic investigation on the mesostructure of structural glass prepared a mechanical examination, which could lead to standard modification.

During the examination we found that the bubble inhomogeneities have a prolate spheroid

shape, with different size, and ratio. The stone had an oblate spheroid form. With the geometrical information we could find analytical solutions on ellipsoidal shape inclusions. With the help of the solutions we can make homogenisation techniques to determine the effect of the inclusions in glass.

Actually the edge finishing has the major effect on the effective strength of the glass, but further procedures (polishing) could repair the imperfections of the surface.

According to the experimental and numerical simulations we can assume that the surface roughness rises during usage. If we treat the glass with acid, the roughness of the new surface could cause as high strain peaks as a grinded edge.

The next step is to continue the numerical simulations of inhomogeneities, and try to calculate a size effect coefficient.

As a conclusion we could say that the mesostructure of the glass has a significant effect on the effective strength of the material,

so it should be taken into account in order to optimize the daily design practice.

Acknowledgements

This work is connected to the scientific program of the "Development of quality-oriented and harmonized R+D+I strategy and functional model at BME" project. This project is supported by the New Hungary Development Plan (Project ID: TÁMOP-4.2.1/B-09/1/KMR-2010-0002).

References

- [1] M. Haldimann, A. Luible, M. Overend: In.: Structural Engineering Document (SED10) IABSE/AIPC/IVBH, Zurich 2008, pp. 85-106.
- [2] G. Molnár, L. G. Vigh, Gy. Stocker, L. Dunai: Per. Polyt. Civil Eng. 56(1) (2012) *in press*
- [3] J.-D. Wörner, J. Schneider, A. Fink: Glasbau. Grundlagen, Berechnungen, Konstruktion (*Glass structure. Bases, Calculations, Contructions*) Springer-Verlag, Berlin-Heidelberg-New York 2001 (*in German*)
- [4] BS EN 1288-3:2000
- [5] C. L. Rountree, S. Prades, D. Bonamya, E. Bouchaud, R. Kalia, C.J. Guillot: J. Alloys and Comp. 434–435 (2007) 60-63.
- [6] W. Kern, D.A. Puotinen: RCA Rev. 31 (1970) 187-206.
- [7] L. Henke, N. Nagy, U.J. Krull: Biosens and Bioelect. 17(6) (2002) 547-555.
- [8] L. M. Molnár, I. Mojzes: In.: Nanotechnológia (*Nanotechnology*), Műegyetem Kiadó, Budapest 2007 (*in Hungarian*).
- [9] G. N. Hounsfield: British J. Radiol. 46 (1973) 1016-1022.